Cancer Imaging

RESEARCH ARTICLE

Open Access

Normal size of benign upper neck nodes on MRI: parotid, submandibular, occipital, facial, retroauricular and level IIb nodal groups

Qi Yong H. Ai[1,2], Tiffany Y. So[2], Kuo Feng Hung[3] and Ann D. King[2*]

Abstract

Purpose: Nodal size is an important imaging criterion for differentiating benign from malignant nodes in the head and neck cancer staging. This study evaluated the size of normal nodes in less well-documented nodal groups in the upper head and neck on magnetic resonance imaging (MRI).

Methods: Analysis was performed on 289 upper head and neck MRIs of patients without head and neck cancer. The short axial diameters (SAD) of the largest node in the parotid, submandibular, occipital, facial, retroauricular and Level IIb of the upper internal jugular nodal groups were documented and compared to the commonly used threshold of ≥ 10 mm for diagnosis of a malignant node.

Results: Normal nodes in the parotid, occipital, retroauricular and Level IIb groups were small with a mean SAD ranging from 3.8 to 4.4 mm, nodes in the submandibular group were larger with a mean SAD of 5.5 mm and facial nodes were not identified. A size ≥ 10 mm was found in 0.8% of submandibular nodes. Less than 10% of the other nodal group had a SAD of ≥ 6 mm and none of them had a SAD ≥ 8 mm.

Conclusion: To identify malignant neck nodes in these groups there is scope to reduce the size threshold of ≥ 10 mm to improve sensitivity without substantial loss of specificity.

Keywords: Normal nodal size, MRI, head and neck, Benign and reactive, Lymph nodes

Background

The spread of head and neck cancer to metastatic nodes in the neck has an important impact on management and prognosis [1–5]. Imaging is used to detect the presence of metastatic nodes and map the extent of disease from the first echelons of nodal spread to subsequent nodal groups down the neck. This information is crucial for neck dissection and radiotherapy field planning and for those cancers treated non-surgically, imaging is the only method to stage the disease [2, 5–7]. The diagnosis of a metastatic node on cross-sectional imaging is dependent on meeting imaging criteria that discriminate malignant nodes from the normal or reactive nodes commonly seen on images of the head and neck [8, 9].

The three main morphological criteria for a malignant node on magnetic resonance imaging (MRI) are size, necrosis and extranodal spread [8, 9]. Of these, the most common feature of a metastatic node is large size, with necrosis and extranodal spread being less commonly encountered [10–12] and therefore of most value in non-enlarged nodes. As malignant nodes tend to be round and reactive nodes oval in shape, the short axis diameter (SAD) on axial images is frequently the measurement of choice [8, 13–15]. The size threshold chosen to detect a malignant node is of course always a trade-off between sensitivity and specificity [8, 16–20] and may

*Correspondence: king2015@cuhk.edu.hk

[2] Department of Imaging and Interventional Radiology, Faculty of Medicine, The Chinese University of Hong Kong, Prince of Wales Hospital, Hong Kong S.A.R, P.R. China

Full list of author information is available at the end of the article

vary between centers and may be influenced by the clinical scenario [21]. However, commonly used thresholds in practice and research are SAD thresholds ≥ 11 mm for the jugulodigastric nodes and ≥ 10 mm for other nodes in the head and neck [8, 22, 23]. The exception is the retropharyngeal nodes where a lower threshold of ≥ 5 or 6 mm is used to reflect the smaller size of normal and reactive nodes in this group [9, 13, 20]. However, benign nodes in the parotid, submandibular, occipital groups and Level IIb of the upper internal jugular group (posterior and separate to the vein) are also usually much smaller than nodes in Level IIa of the upper internal jugular group (adjacent to the vein), but the normal size range of these nodal groups is poorly documented in the literature. Furthermore, nodes in facial and retroauricular groups are rarely observed. Using the threshold of 10 mm in these groups could reduce sensitivity for metastatic nodal spread from head and neck cancers that drain to these sites. The lower frequency of metastatic nodes in these groups, compared to those along the internal jugular chain, make it difficult to obtain sufficient data from surgical series to define optimum size thresholds to divide malignant from benign nodes. A study of nodal size in patients without head and neck cancer should at least shed light on the expected upper limit of size of normal/reactive benign nodes.

In this study we documented the expected range of size for benign nodes in the parotid, submandibular, occipital, Level IIb, facial and retroauricular groups by measuring the SAD of the largest nodes in these groups on the upper neck MRI images of patients without cancer. We also measured the SAD of the already well-documented nodes in the upper internal jugular (jugulodigastric and other Level IIa) and retropharyngeal groups, to compare the size of these nodes in our cohort with those previously reported in the literature. Finally, for each nodal group we documented the frequency of nodes, correlated the size of the largest node with age and measured nodal sizes in both sides of the neck to determine the expected discrepancy between the right and the left sides of the neck.

Methods

Patients

This retrospective study was performed with approval from the local institutional review board and written informed consent was waived. This study analysed 289 upper head and neck MRI scans of patients who were referred to our institution between 2005 and 2016 for suspected NPC due to the raised plasma Epstein-Barr Virus (EBV)-DNA but who had no head and neck cancer diagnosed at a minimum follow-up of 2 years. The median age of the included patients was 53 years (range: 28 -78 years).

MRI acquisition

The upper head and neck MRI was performed using a 1.5 T or 3 T whole-body MRI system (Philips Healthcare, Best, the Netherlands) and comprised of at least (1) axial fat-suppressed T2-weighted (repetition time/ echo time, 2500—4000/ 80—100 ms; field of view, 22 cm; section thickness, 4 mm without a slice gap; number of slices, 30; echo train length, 15–17; sensitivity encoding factor, 1; number of signal acquired, 2), (2) axial T1-weighted images (repetition time/ echo time, 500/ 10—20 ms; field of view, 22 cm; section thickness, 4 mm without a slice gap; number of slices, 30; echo train length, 4; sensitivity encoding factor, 1; number of signal acquired, 2) with or without (3) coronal T2- or T1-weighted images, and (4) contrast-enhanced axial T1-weighted images.

MRI analysis

Nodal groups based on sites described by Som et al. and Gregoire et al. [22–24] were examined, comprising six less documented groups which were (1) parotid, (2) submandibular, (3) occipital, (4) Level IIb, (5) facial and (6) retroauricular (Fig. 1a-e), together with (7) retropharyngeal, (8) jugulodigastric region and (9) Level IIa (other than the jugulodigastric node) (Fig. 2a-b). The SAD of the largest node in each group was measured on the MRI images in the axial plane. Only nodes ≥ 2.0 mm in SAD were considered to be measurable and included in the study. Nodal size was documented using the SAD by a researcher with 7 years experiences in head and neck imaging. Measurements were also performed for inter-observer assessment on 50 randomly selected MRIs by a radiologist with 3 years of experiences in head and neck radiology.

Statistical analysis

For each nodal group, frequency of nodes was based on patients who had a node in either side of the neck and the SAD was based on the size of the largest node. For patients with bilateral nodes, the paired t-test (data normally distributed) or Wilcoxon signed-rank test (data non-normally distributed) compared the differences in the SAD of the largest node in each nodal group between the right and left sides of the neck. For patients with unilateral nodes, the student t-test (data normally distributed) or Mann–Whitney test (data non-normally distributed) compared differences in SAD of the largest node in each group with the size of the largest node in those with bilateral nodes. The normality distribution of data was evaluated using Kolmogorov–Smirnov test. The SAD of the largest node in each nodal group was

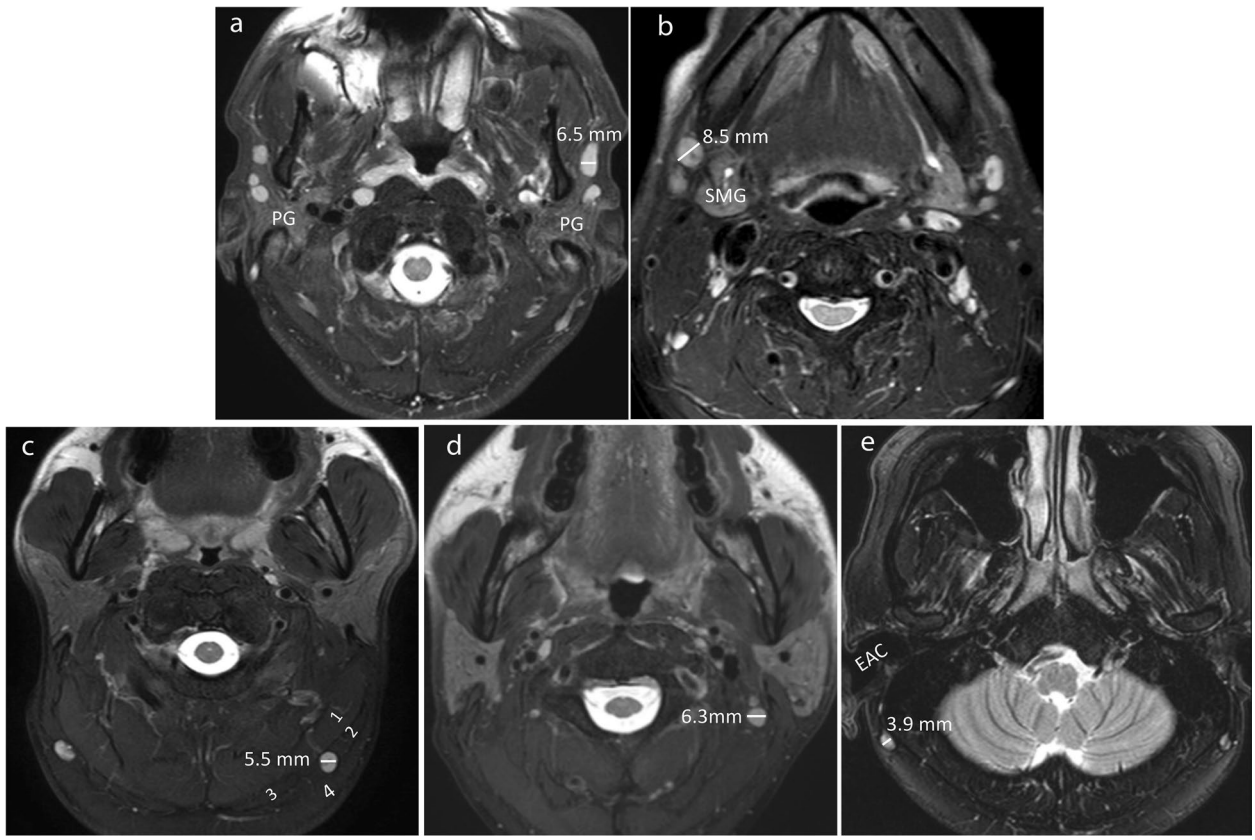

Fig. 1 Axial T2-weighted fat-suppressed MR images of five patients without head and neck cancer with normal/benign reactive nodes in the less documented nodal groups in the upper head and neck, comprising parotid (**a**), submandibular (**b**), occipital (**c**), Level IIb (**d**) and retroauricular nodes (**e**). The mean SADs of the largest nodes for parotid, submandibular, occipital, Level IIb, and retroauricular nodes were 4.4 ± 1.0 mm, 5.5 ± 1.4 mm, 3.8 ± 1.0 mm, 4.3 ± 1.2 mm, and 3.8 ± 0.7 mm, respectively. (PG = parotid gland, SMG = submandibular gland, EAC = external auditory canal, SAD = short axis diameter, 1 = Splenius capitis muscle, 2 = sternocleidomastoid muscle, 3 = trapezius muscle, 4 = occipital subcutaneous fat)

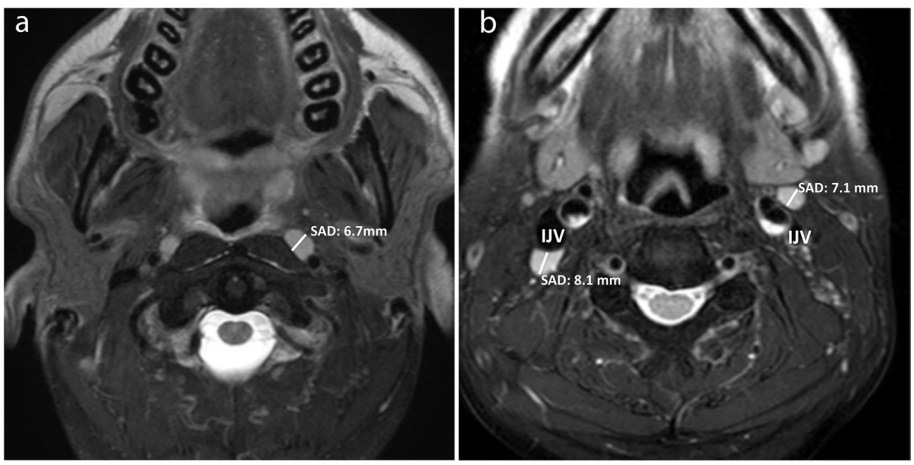

Fig. 2 Axial T2-weighted fat-suppressed MR images of two patients without head and neck cancer showing bilateral normal/benign reactive retropharyngeal (**a**), left jugulodigastric (**b**) and right Level IIa (**b**) nodes. The mean SADs of the largest nodes for retropharyngeal, jugulodigastric, and Level IIa nodes were 3.9 ± 1.2 mm, 7.4 ± 1.9 mm, and 4.9 ± 1.6 mm, respectively. (IJV = internal jugular vein, SAD = short axis diameter)

correlated with age using the Pearson correlation test and the Pearson coefficient was calculated. All statistical tests were 2-sided, and a p-value < 0.05 was considered to indicate a statistically significant difference. Analyses were performed using the statistical analysis software SPSS (version 26.0; IBM). Inter-observer agreement for the SAD of the largest node in each nodal group were evaluated using the intra-class correlation test and the intra-class coefficient (ICC) was calculated.

Results

Frequency of patients with the nodes in each nodal group

The frequencies of nodes in descending order were the jugulodigastric (98.2%) > submandibular (90.3%) > Level IIa (81.6%) > Level IIb (79.2%) > parotid (74.4%) > retropharyngeal (49.1%) > occipital (27.7%) > retroauricular (2.8%) (Table 1). Nodes were not identified in facial group (Table 1). For the parotid group, 80.0% (172/215) of the largest nodes were in the superficial lobe of which 68.0% (117/172) were at a constant location in the anterior portion (Fig. 1a), 20.0% (43/215) were in the deep lobe.

Size of the largest nodes in each nodal group

The SADs of the largest nodes in descending order were jugulodigastric (7.4 ± 1.9 mm) > submandibular (5.5 ± 1.4 mm) > Level IIa (4.9 ± 1.6 mm) > parotid (4.4 ± 1.0 mm) > Level IIb (4.3 ± 1.2 mm) > retropharyngeal nodes (3.9 ± 1.2 mm) > occipital nodes (3.8 ± 1.0 mm) and retroauricular nodes (3.8 ± 0.7 mm) (Table 1). The range of size of nodes in each group is shown in Supplementary Table 1. The percentage of benign nodes larger than the current thresholds for a malignant node were 15.5% (22/142) for retropharyngeal, 5.3% (15/284) for jugulodigastric, 1.3% (3/236) for Level IIa and 0.8% (2/261) for submandibular groups (Table 1). Less than 10% of nodes in the parotid, occipital, Level IIb, retropharyngeal and retroauricular groups had a SAD of ≥ 6 mm and none of the nodes in the parotid, occipital, Level IIb, and retroauricular groups had a SAD ≥ 8 mm (Supplementary Table 1).

Comparison of size of nodes in each side of the neck

The SAD of the largest node in each group was significantly smaller when nodes were unilateral compared to bilateral (p < 0.01 to 0.048, Table 2) but for bilateral nodes there was no significant difference between the right and left sides (p = 0.14 to 0.92) (Table 3).

Correlation of nodal size in each group with age

Age negatively correlated with the SAD of the largest node in the retropharyngeal and upper internal jugular group (jugulodigastric nodes, Level IIa, and Level IIb nodes) (Pearson correlation coefficients: -0.19 to -0.15,

Table 1 Frequency and SAD of the largest node in each nodal group

Nodal groups	Frequency of patients with nodes	SAD[a] (mm)	Number (percentage) of nodes with a SAD > current size criteria for a malignant node[b]
Parotid	215 (74.4%)	4.4 ± 1.0 (2.2 – 7.3)	0 (0%)
Submandibular	261 (90.3%)	5.5 ± 1.4 (2.7 – 10.8)	2 (0.8%)
Occipital	80 (27.7%)	3.8 ± 1.0 (2.1 – 6.1)	0 (0%)
Facial	0 (0%)	0 (-)	0 (0%)
Retroauricular	8 (2.8%)	3.8 ± 0.7 (3.3 – 4.8)	0 (0%)
Retropharyngeal	142 (49.1%)	3.9 ± 1.2 (2.1 – 9.0)	22 (15.5%)
Upper internal jugular			
Jugulodigastric	284 (98.2%)	7.4 ± 1.9 (2.8 – 12.6)	15 (5.3%)
Level IIa	236 (81.6%)	4.9 ± 1.6 (2.3 – 11.9)	3 (1.3%)
Level IIb	229 (79.2%)	4.3 ± 1.2 (2.1– 7.6)	0 (0%)

SAD Short axis diameter

[a] data shown as mean value ± standard deviation (range)

[b] SAD of ≥ 5 mm, 11 mm, and 10 mm for identifying malignant retropharyngeal nodes, jugulodigastric nodes, and any other head and neck nodes respectively

Table 2 Frequency and SAD of the largest node in patients with unilateral and bilateral nodes

Nodal groups	Number of patients with unilateral nodes	Number of patients with bilateral nodes	SAD of the largest node		
			Unilateral*	Bilateral*	*P*-value
Parotid	81 (28.0%)	134 (46.4%)	4.1 ± 1.0	4.6 ± 0.9	< 0.01
Submandibular	57 (19.7%)	204 (70.6%)	4.7 ± 1.2	5.7 ± 1.4	< 0.01
Occipital	58 (20.1%)	22 (7.6%)	3.6 ± 0.9	4.1 ± 1.0	0.048
Retroauricular	8 (2.8%)	0 (0%)	3.8 ± 0.7	-	-
Retropharyngeal	59 (20.4%)	83 (28.7%)	3.5 ± 0.9	4.2 ± 1.3	< 0.01
Upper internal jugular					
Jugulodigastric	20 (6.9%)	264 (91.3%)	6.1 ± 1.9	7.5 ± 1.9	< 0.01
Level IIa	79 (27.3%)	157 (54.3%)	4.2 ± 1.1	5.3 ± 1.6	< 0.01
Level IIb	56 (19.4%)	173 (59.8%)	3.7 ± 1.1	4.5 ± 1.1	< 0.01

All data groups are normally distributed ($p > 0.05$ using one sample Kolmogorov–Smirnov test)

SAD Short axis diameter

* data shown as mean value ± standard deviation

Table 3 The SAD of the largest node in the left and right side in patients with bilateral nodes in the same group[a]

Nodal groups	SAD in patients with bilateral nodes		
	Left	Right	*P*-value
Parotid ($n = 134$)	4.2 ± 0.9	4.1 ± 1.0	0.19
Submandibular ($n = 204$)	5.0 ± 1.5	5.0 ± 1.5	0.92
Occipital ($n = 22$)	3.8 ± 1.1	3.9 ± 1.2	0.71
Retropharyngeal ($n = 83$)	3.9 ± 1.1	3.7 ± 1.2	0.14
Upper internal jugular			
Jugulodigastric ($n = 264$)	6.7 ± 2.0	6.8 ± 1.9	0.36
Level IIa ($n = 157$)	4.7 ± 1.6	4.5 ± 1.6	0.14
Level IIb ($n = 173$)	4.0 ± 1.2	4.0 ± 1.1	0.86

All data groups are normally distributed ($p > 0.05$ using one sample Kolmogorov–Smirnov test)

SAD short axis diameter

[a] No patients with facial or retroauricular nodes had bilateral nodes

$p < 0.01$ to 0.02) (Supplementary Fig. 1), but not with parotid, submandibular, occipital and retroauricular nodes ($p = 0.09$ to 0.57) (Table 4).

Inter-observer agreement

Inter-observer agreement for SAD of the largest nodes in the nodal groups showed ICCs ranged from 0.82 to 0.93 (all $p < 0.01$) (Supplementary Table 2).

Table 4 Correlation of age with SAD of the largest nodes in each nodal group[a]

Nodal groups	SAD[b] (mm)	Pearson Coefficient	*P*-value
Parotid	4.4 ± 1.0 (2.2 – 7.3)	-0.12	0.09
Submandibular	5.5 ± 1.4 (2.7 – 10.8)	-0.10	0.12
Occipital	3.8 ± 1.0 (2.1 – 6.1)	-0.11	0.57
Retroauricular	3.8 ± 0.7 (3.3 – 4.8)	-0.12	0.13
Retropharyngeal	3.9 ± 1.2 (2.1 – 9.0)	-0.19	**0.02**
Upper internal jugular			
Jugulodigastric	7.4 ± 1.9 (2.8 – 12.6)	-0.18	**< 0.01**
Level IIa	4.9 ± 1.6 (2.3 – 11.9)	-0.15	**0.02**
Level IIb	4.3 ± 1.2 (2.1– 7.6)	-0.16	**0.01**

SAD Short axis diameter

[a] No patient had facial nodes

[b] data shown as mean value ± standard deviation (range)

Discussion

This study documented the frequency and range in size of normal/reactive benign nodes in nodal groups of

head and neck that have received less scrutiny in the literature, namely the parotid, submandibular, occipital, Level IIb nodes, facial and retroauricular groups. Measurable nodes (i.e., those ≥ 2 mm) were most frequent in the submandibular (90.3%), followed by Level IIb (79.2%), parotid (74.4%), occipital (27.7%) and retroauricular (2.8%) groups, and no nodes were identified in the facial group. Nodes in the parotid, occipital, Level IIb, and retroauricular groups were small ranging in mean SAD from 3.8 to 4.4 mm, while nodes in the submandibular group were slightly larger with a mean SAD of 5.5 mm. The range of nodal size in each of these groups only surpassed the threshold of ≥ 10 mm for a malignant node in 0.8% of submandibular nodes and none of the nodes in the other groups.

Nodal sizes for retropharyngeal, jugulodigastric and other Level IIa nodes were in keeping with sizes reported in the literature, suggesting our group is fairly representative of the expected size of normal/reactive nodes [8, 9, 13, 25, 26]. Of note, the largest node in the neck was the jugulodigastric node followed by the other Level IIa nodes. The larger size of jugulodigastric, Level IIa and submandibular nodes may reflect stimulation by dental disease or upper respiratory tract infections. The size of the retropharyngeal nodes was similar to nodes in the parotid, Level IIb, occipital groups and retroauricular groups. The smaller nodal size in the upper internal jugular chain in Level IIb compared to Level IIa, is of special interest in these patients being screened for NPC, because Level IIb nodes are commonly the first echelon of nodal spread in NPC [27]. The results in this study suggest that applying the current threshold of ≥ 10 mm to parotid, occipital, Level IIb nodes, facial and retroauricular nodes would result in a very high specificity for a malignant node but would compromise sensitivity. Recently Elsholtz et al. [28], proposed using a threshold of < 5 mm to denote normal nodes in the facial, parotid, retroauricular, occipital groups for a Node-RADS system that categorises the likelihood of a metastatic node from 1 to 5. Our findings support lowering the threshold from 10 mm to one that is similar to that already applied to retropharyngeal nodes, i.e., 5 mm or 6 mm [9, 13, 20]. Our current results suggest that 6 mm, rather than 5 mm, would reduce the number of false positive nodes and improve specificity in the parotid, occipital, Level IIb nodes, as well as the retropharyngeal group. However, thresholds may need to be adjusted 1- 2 mm higher or lower for submandibular and retroauricular groups respectively and the presence of any node in the facial group. Moreover, size thresholds are a trade-off between sensitivity and specificity and chosen thresholds may need to be adapted to the clinical scenario; for example to improve sensitivity when searching for small metastases in surgical candidates with a clinically N0 neck, thresholds as low as ≥ 4 mm [17, 29, 30] may be used for ultrasound guided fine needle aspiratory cytology of submandibular and upper internal jugular nodes.

Unilateral nodes or nodes larger on one side than the other is often used as a sign to heighten suspicion of a metastatic node in groups along the expected pathway of nodal spread. The results of this study support this practice for unilateral nodes, especially in the jugulodigastric region where only 6.9% were unilateral, compared to 19–28% in the other nodal groups. Interestingly, when nodes were bilateral, they were larger than when unilateral which may represent a general stimulation of nodes, in our group this may possibly be due to EBV infection causing reactive nodes. However, once nodes were bilateral nodes there was no significant difference in size between the right and left sides of the neck, again suggesting that asymmetry in size should be regarded with suspicion.

This study found age negatively correlated with the SAD of nodes in retropharyngeal group, and upper jugular group (jugulodigastric nodes, Level IIa and Level IIb nodes) as shown in previous studies [25, 31]. However, we found no correlation between age and size of nodes in the parotid, submandibular and occipital groups.

Although this study has focused on size criterion, it is worth remembering that the imaging diagnosis of a metastatic node, especially for those small nodes that do not surpass the size threshold, also takes account of other morphological features such as shape, necrosis, heterogeneity, extranodal spread, hilum, vascular pattern and functional features such as F-fluorodeoxyglucose activity and restricted diffusion.

There are some limitations in this study. First, evaluation of nodal groups was limited to those groups consistently covered in all scans of the upper neck, which unfortunately did not include submental nodes. Second, this study only evaluated measurable nodes (a SAD of ≥ 2 mm) which may result in under reporting of the frequency of the nodes in each nodal group. However, this assured the certainty in identifying a node rather than other structures (i.e., small vessels). Third, all patients in this study were from a single institution but this group should represent the expected range in size of benign nodes (normal and reactive). Although this group of patients with persistently elevated plasma EBV-DNA may have a potential bias towards reactive, and hence larger size, benign nodes, this adds to strength to the findings that a reduction in nodal size threshold for detecting malignant nodes should not compromise specificity. Fourth, the influence of outliers on the statistical significance between age and SAD is unknown. Fifth, the diagnostic performance of the SAD thresholds could not

be fully assessed because we only evaluated the SAD of benign and not metastatic nodes. Radiology studies that include both malignant and benign nodes with pathological correlation are needed to explore the diagnostic performance of size thresholds for these under reported nodal groups, and this may require multicenter studies as data from a single center may be insufficient for analysis.

Conclusion

This study examined the frequency and size of benign nodes in the parotid, submandibular, occipital, level IIb, facial and retroauricular nodes in the upper neck. Most patients had nodes in each of these groups on imaging, with the exception of the facial group. Nodes in these groups were small (mean SAD ranging from 3.8 to 4.4 mm) while nodes in the submandibular group were slightly larger (mean SAD of 5.5 mm).

Reducing the size threshold of nodes in the head and neck is known to improve sensitivity for identifying malignant nodes in the head and neck and our results suggest this may be possible without substantial loss of specificity in these less well documented nodal groups. Our data should encourage future investigation of sensitivity and specificity using a lower threshold for detection of malignant nodes (i.e., $\geq$ 6–7 mm for parotid, occipital and Level IIb groups or 1–2 mm higher for submandibular group or lower for retroauricular group). Results also support heighten suspicion of metastatic nodes when nodes in groups along the expected pathway of nodal spread are unilateral or larger on one side than the other.

Abbreviations

MRI: Magnetic resonance imaging; SAD: Short axis diameter; NPC: Nasopharyngeal carcinoma; EBV: Epstein-Barr virus; DNA: Deoxyribonucleic acid; ICC: Intra-class coefficient; PG: Parotid gland; SMG: Submandibular gland; IJV: Internal jugular vein.

Supplementary Information

The online version contains supplementary material available at https://doi.org/10.1186/s40644-022-00504-z.

Additional file 1: Supplementary Table 1. Frequency of the nodes according to range in SAD of the largest node*. **Supplementary Table 2.** Inter-observer agreement for SAD of the largest nodes*. **Supplementary Figure 1.** Scatter plots show the negative correlation of age with the short axis diameter of the largest node inretropharyngeal (a), jugulodigastric (b), Level IIa (c) and Level IIb (d) nodes. The Pearson correlation coefficients are -0.19, -0.18, -0.15, and -0.16 for retropharyngeal, jugulodigastric, Level IIa and Level IIb nodes,respectively.

Acknowledgements

Not applicable.

Authors' contributions

Conception: ADK; study design: QYHA and ADK; data collection: QYHA; data analysis: QYHA,TYS, and KFH; data interpretation: QYHA and ADK, manuscript writing: QYHA and ADK; manuscript editing: All authors. The author(s) read and approved the final manuscript.

Funding

This study was partially supported by The Start-up Fund for RAPs under the Strategic Hiring Scheme funded by The Hong Kong Polytechnic University. (Ref. P0039027).

Availability of data and materials

The datasets of current study are available from the corresponding author on reasonable request.

Declarations

Ethics approval and consent to participate

This retrospective study was performed with approval from The Joint Chinese University of Hong Kong – New Territories East Cluster Clinical Research Ethics Committee (CRE-2011.464) and written informed consent was waived.

Consent for publication

Not applicable.

Competing interests

All authors declare no competing interests.

Author details

[1]Department of Health Technology and Informatics, The Hong Kong Polytechnic University, Hong Kong S.A.R, P.R. China. [2]Department of Imaging and Interventional Radiology, Faculty of Medicine, The Chinese University of Hong Kong, Prince of Wales Hospital, Hong Kong S.A.R, P.R. China. [3]Division of Oral and Maxillofacial Surgery, Faculty of Dentistry, University of Hong Kong, Hong Kong S.A.R, P.R. China.

Received: 26 August 2022 Accepted: 10 November 2022
Published online: 08 December 2022

References

1. Klausner G, Troussier I, Blais E, Carsuzaa F, Zilli T, Miralbell R, et al. Neck management in head and neck squamous cell carcinomas: where do we stand? Med Oncol. 2019;36(5):40.
2. Hamoir M, Schmitz S, Gregoire V. The Role of Neck Dissection in Squamous Cell Carcinoma of the Head and Neck. Curr Treat Options Oncol. 2014;15:611–24.
3. Ai Q-YH, Hung KF, So TY, Mo FKF, Tsung Anthony Chin W, Hui EP, et al. Prognostic value of cervical nodal necrosis on staging imaging of nasopharyngeal carcinoma in era of intensity-modulated radiotherapy: a systematic review and meta-analysis. Cancer Imaging. 2022;22(1):24.
4. Tsai TY, Chou YC, Lu YA, Kang CJ, Huang SF, Liao CT, et al. The prognostic value of radiologic extranodal extension in nasopharyngeal carcinoma: Systematic review and meta-analysis. Oral Oncol. 2021;122: 105518.
5. Biau J, Lapeyre M, Troussier I, Budach W, Giralt J, Grau C, et al. Selection of lymph node target volumes for definitive head and neck radiation therapy: a 2019 Update. Radiother Oncol. 2019;134:1–9.
6. King AD. MR Imaging of Nasopharyngeal Carcinoma. Magn Reson Imaging Clin N Am. 2022;30(1):19–33.
7. Lin L, Lu Y, Wang XJ, Chen H, Yu S, Tian J, et al. Delineation of Neck Clinical Target Volume Specific to Nasopharyngeal Carcinoma Based on Lymph Node Distribution and the International Consensus Guidelines. Int J Radiat Oncol Biol Phys. 2018;100:891–902.
8. van den Brekel M, Stel H, Castelijns J, Nauta J, van der Waal I, Valk J, et al. Cervical lymph node metastasis: assessment of radiologic criteria. Radiology. 1990;177:379–84.
9. King AD, Ahuja AT, Leung SF, Lam WWM, Teo P, Chan YL, et al. Neck node metastases from nasopharyngeal carcinoma: MR imaging of patterns of disease. Head Neck. 2000;22:275–81.
10. King AD, Tse GMK, Ahuja AT, Yuen EHY, Vlantis AC, To EWH, et al. Head and Neck Imaging Radiology Necrosis in Metastatic Neck Nodes : Diagnostic Accuracy of CT, MR Imaging, and US. Radiology. 2004;230:720–6.

11. Mao YP, Liang SB, Liu LZ, Chen Y, Sun Y, Tang LL, et al. The N staging system in nasopharyngeal carcinoma with radiation therapy oncology group guidelines for lymph node levels based on magnetic resonance imaging. Clin Cancer Res. 2008;14:7497–503.
12. Mermod M, Tolstonog G, Simon C, Monnier Y. Extracapsular spread in head and neck squamous cell carcinoma: A systematic review and meta-analysis. Oral Oncol. 2016; 62:60–71.
13. Zhang GY, Liu LZ, Wei WH, Deng YM, Li YZ, Liu XW. Radiologic criteria of retropharyngeal lymph node metastasis in nasopharyngeal carcinoma treated with radiation therapy. Radiology. 2010;255:605–12.
14. Wang Y, Mao M, Li J, Feng Z, Qin L, Han Z. Diagnostic value of magnetic resonance imaging in cervical lymph node metastasis of oral squamous cell carcinoma. Oral Surg Oral Med Oral Pathol Oral Radiol. 2022;133:582–92.
15. Kosugi Y, Suzuki M, Fujimaki M, Ohba S, Matsumoto F, Muramoto Y, et al. Radiologic criteria of retropharyngeal lymph node metastasis in maxillary sinus cancer. Radiat Oncol. 2021;16:190.
16. Curtin HD, Mancuso AA, Dailey RW, Caudry DJ, Mcneil BJ. Comparison of CT and MR imaging in staging of neck metastases. Radiology. 1998;207:123–30.
17. van den Brekel MWM, Castelijns JA, Snow GB. The Size of Lymph Nodes in the Neck on Sonograms as a Radiologic Criterion for Metastasis: How Reliable Is It? Am J Neuroradiol. 1998;19:695–700.
18. van den Brekel MWM, Castelijns JA, Stel Hv, Golding RP, Meyer CJL, Snow GB. Modern imaging techniques and ultrasound-guided aspiration cytology for the assessment of neck node metastases: a prospective comparative study. Eur Arch Otorhinolaryngol. 1993;250:11–7.
19. Steinkamp HJ, Hosten N, Richter C, Schedel H, Felix R, Berlin U, et al. Enlarged Cervical Lymph Nodes at Helical CT. Radiology. 1994;191:795–8.
20. Tu DG, Chen HY, Yao WJ, Hung YS, Chang YK, Chang CH, et al. Verification of the efficacy of new diagnostic criteria for retropharyngeal nodes in a cohort of nasopharyngeal carcinoma patients. Int J Med Sci. 2021;18:3463–9.
21. Kelly HR, Curtin HD. Chapter 2 Squamous Cell Carcinoma of the Head and Neck—Imaging Evaluation of Regional Lymph Nodes and Implications for Management. Seminars in Ultrasound, CT and MRI. 2017;38:466–78.
22. Som PM. Detection of Metastasis in Cervical Lymph Nodes: CT and MR Criteria and Differential Diagnosis. American Journa of Roentgenology. 1992;158:961–9.
23. Som PM, Curtin HD, Mancuso AA. Imaging-Based Nodal Classification for Evaluation of Neck Metastatic Adenopathy. Am J Roentgenol. 2000;174:837–44.
24. Grégoire V, Ang K, Budach W, Grau C, Hamoir M, Langendijk Ja, et al. Delineation of the neck node levels for head and neck tumors: A 2013 update. DAHANCA, EORTC, HKNPCSG, NCIC CTG, NCRI, RTOG, TROG consensus guidelines. Radiother Oncol. 2014;110:172–81.
25. Costa e Silva Souza LMB, Leung KJ, O'Neill A, Jayender J, Lee TC. Jugulodigastric lymph node size by age on CT in an adult cancer-free population. Clin Imaging. 2018;47:30–3.
26. Kato H, Kanematsu M, Watanabe H, Mizuta K, Aoki M. Metastatic retropharyngeal lymph nodes: Comparison of CT and MR imaging for diagnostic accuracy. Eur J Radiol. 2014;83:1157–62.
27. Wang X, Hu C, Ying H, He X, Zhu G, Kong L, et al. Patterns of lymph node metastasis from nasopharyngeal carcinoma based on the 2013 updated consensus guidelines for neck node levels. Radiother Oncol. 2015;115:41–5.
28. Elsholtz FHJ, Asbach P, Haas M, Becker M, Beets-Tan RGH, Thoeny HC, et al. Introducing the Node Reporting and Data System 1.0 (Node-RADS): a concept for standardized assessment of lymph nodes in cancer. Eur Radiol. 2021;31:6116–24.
29. de Bondt RBJ, Nelemans PJ, Hofman PAM, Casselman JW, Kremer B, van Engelshoven JMA, et al. Detection of lymph node metastases in head and neck cancer: A meta-analysis comparing US, USgFNAC, CT and MR imaging. Eur J Radiol. 2007;64:266–72.
30. Richards PS, Peacock TE. The role of ultrasound in the detection of cervical lymph node metastases in clinically NO squamous cell carcinoma of the head and neck. Cancer Imaging. 2007;7:167–78.
31. Alves Rosa J, Calle-Toro JS, Kidd M, Andronikou S. Normal head and neck lymph nodes in the paediatric population. Clin Radiol. 2021;76:315.e1-315.e7.

Publisher's Note